

Wide-angle and broadband graded-refractive-index antireflection coatings

Zhang Jun-Chao(张俊超)^{a)b)†}, Xiong Li-Min(熊利民)^{a)}, Fang Ming(方明)^{b)}, and He Hong-Bo(贺洪波)^{b)}

^{a)}Optic and Laser Division, National Institute of Metrology, Beijing 100013, China

^{b)}Key Laboratory of Material Science and Technology for High Power Lasers, Shanghai Institute of Optics and Fine Mechanics, Chinese Academy of Sciences, Shanghai 201800, China

(Received 21 July 2012; revised manuscript received 9 September 2012)

The design and fabrication of graded-refractive-index (GRIN) antireflection (AR) coatings with wide-angle and broadband characteristics are demonstrated. The optimization of the graded-index profiles with a genetic algorithm is used in the design of the GRIN AR coatings. The average reflectance over a wavelength range from 400 nm to 800 nm and angles of incidence from 0° to 80° could be reduced to only 0.1% by applying an optimized AR coating onto BK7 glass. The optimization of step-graded GRIN AR coating is then further investigated in detail. A two-layer AR coating was deposited by electron beam evaporation with glancing angle deposition technology, and the positional homogeneity was improved by depositing the film from two opposite directions. The microstructure of the AR coating was investigated by scanning electron microscopy, and the residual reflectances of the coating sample are in agreement with theoretical calculations. The optimized GRIN AR coatings are beneficial to increasing the efficiency of light utilization.

Keywords: antireflection, wide-angle, broadband, refractive-index profile

PACS: 42.25.Gy, 42.79.Ry, 42.79.Wc

DOI: 10.1088/1674-1056/22/4/044201

1. Introduction

Antireflection (AR) coatings are an important part of many devices and are used widely in optical systems. These coatings can be divided into two types: homogeneous and inhomogeneous films. The former reduce reflection losses by destructive interference with light reflected from various interfaces.^[1] A single layer AR coating with an optical thickness equal to one-quarter of the wavelength of interest ($\lambda/4$) is widely used. The refractive index of such an AR coating is given by

$$n_{\lambda/4} = (n_s n_a)^{1/2}, \quad (1)$$

where n_s and n_a are the refractive indices of the substrate and ambient medium, respectively.^[2] However, such quarter-wave coating cannot present very good performance for wide angle and wide wavelength ranges. The inhomogeneous AR coatings or graded-refractive-index (GRIN) AR coatings^[3,4] whose refractive indices vary gradually, can effectively reduce the surface reflection by matching the refractive indices of the substrate and ambient medium. These coatings with omnidirectional and broadband characteristics can potentially satisfy the requirements of many fields, such as solar cells. Many forms of gradient profiles^[5-9] have been studied previously. Kuo *et al.* fabricated a seven-layer graded-index coating with quintic profiles.^[10] The measured angle- and wavelength-averaged total reflectance was 3.79% for wavelengths between

400 nm and 2000 nm and for incident angles between 8° and 60°. However, AR performance gets worse at large angles of incidence. In recent years, the optimization method has been applied to the design of broadband omnidirectional step-graded GRIN AR coatings. A three-layer AR coating on a silicon substrate was designed using the iterative genetic algorithm computational method.^[11] Reflectances were reduced to 5.9% over the wavelength range from 400 nm to 1100 nm and at angles of incidence from 0° to 90°.

Among various preparation methods of GRIN coatings, such as multi-source co-deposition,^[12] reactive magnetron sputtering^[13] and so on, the glancing angle deposition (GLAD) technique^[14,15] is an effective method to grow nanostructured thin-film materials with engineered nano-scale porosity variations. Compared with other deposition methods, GLAD can obtain some materials with refractive indices close to that of air, which is crucial for the fabrication of broadband and omnidirectional GRIN antireflection coatings. A very low refractive index of 1.05 nm at 632.8 nm was reported for SiO₂ grown by GLAD using electron-beam evaporation.^[16] Thus, this technique is applied widely in the deposition of GRIN AR coatings.

In this paper, we present a design method for wide-angle and broadband AR coatings by optimizing the gradient profile of the refractive index. The reflectances of optimized step-graded GRIN antireflection coatings varying with the discrete numbers of layers have been studied. We also analyzed the

[†]Corresponding author. E-mail: zhangjunchao4568@163.com

relationship between the effective refractive index of porous SiO₂ and glancing angle. An optimized two-step GRIN AR coating on a BK7 substrate was prepared by electron beam evaporation with the GLAD technique. The measured results demonstrate that the antireflection performance of the two-layer AR coating with a simple structure is excellent.

2. Design method and results

2.1. Optimization of the refractive-index profile

The remarkable feature of GRIN AR coating is that the refractive index varies gradually and monotonically along its thickness from the refractive index of the ambient medium to that of the substrate. Some specific gradient profiles, such as Gaussian, quintic, sinusoidal, exponential, and exponential-sine, have been adopted in designing GRIN AR coatings. In order to design GRIN AR coatings, we optimized the refractive-index profiles by an iterative genetic algorithm computational method,^[17–19] which has previously been applied to the optimization of a variety of optical coatings. The details of the genetic algorithm have been discussed in previous papers.^[20]

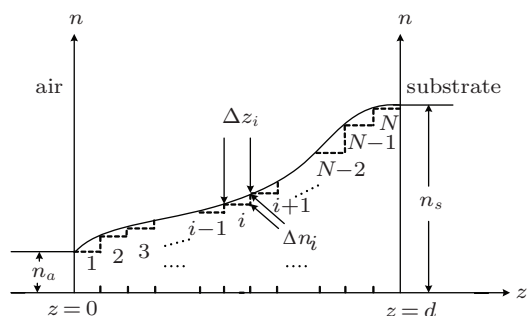


Fig. 1. Schematic drawing of the optimization of the GRIN profile.

In the design procedure, the GRIN AR structure is modeled by an N -layer homogeneous sublayer system, whose refractive-index profile is shown in Fig. 1. The total number of sublayers is set at 500. It is found that the larger the total thickness of the GRIN AR coating, the lower the resulting average reflectance gets. In the following, the physical thickness (d) of the graded-index coating is considered to be 0.8 μm . The refractive indices of the sublayers increase monotonically with the layer number (position) from the air side to the substrate side. The thickness (Δz_i) of every sublayer and the difference in refractive index (Δn_i) between adjacent sublayers are all optimized. Then the refractive-index profile is optimized indirectly. A merit function (MF), defined as the average reflectance used in the process, is given by

$$\text{MF} = \frac{1}{m * n} \sum_{j=1}^m \sum_{i=1}^n \frac{R_s(\lambda_i, \theta_j) + R_p(\lambda_i, \theta_j)}{2}, \quad (2)$$

where $R_s(\lambda_i, \theta_j)$ and $R_p(\lambda_i, \theta_j)$ are the wavelength and the angle-dependent reflection for s- and p-polarizations, respectively. m and n are the sampling numbers of the angles and wavelengths over the design ranges, respectively. Wide-angle AR coatings over the entire visible wavelength range are widely used in many fields, such as light-emitting diodes (LED). In order to simplify the optimization process, the wavelengths (λ_i) and angles (θ_j) are adopted separately from 400 nm to 800 nm at 25 nm steps and 0° to 80° at 5° steps. The substrate we used in the design process is BK7 glass ($n_s = 1.52$) and the ambient medium is air ($n_a = 1.0$). In this study, the dispersion of optical constants is not added into our calculations. Figure 2 illustrates the refractive-index profile and the AR-behavior of an optimized coating. The average reflectance over the wavelength range from 400 nm to 800 nm and the 0°–80° angle of incidence is only 0.1%.

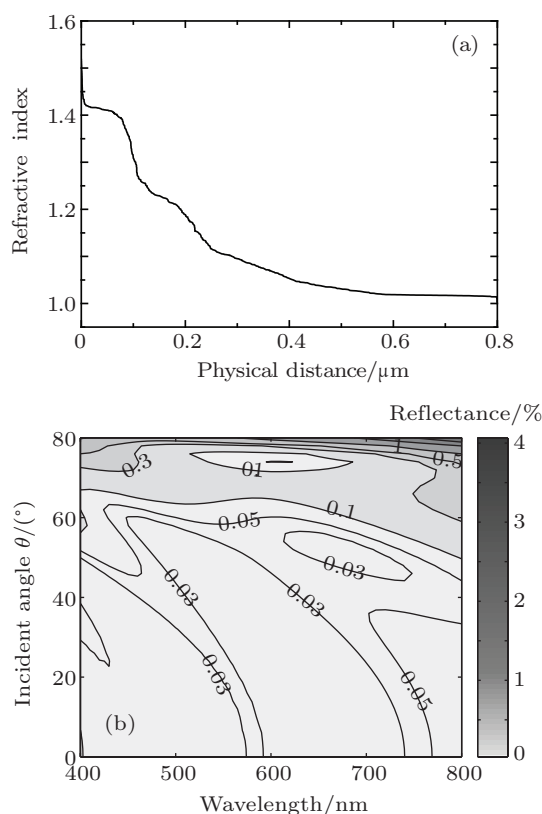


Fig. 2. (a) Refractive index profile and (b) reflection characteristics of the optimized GRIN AR coating.

Figure 3 shows the reflectances of a continuous quintic AR coating and of the optimized GRIN AR coating, both averaged over the wavelength range of 400 nm–800 nm as a function of incident angle. It can be seen that the quintic coating reduces average reflectance remarkably when the angle is less than about 55°, but the AR performance becomes worse rapidly once the incident angle goes above 55°. The reflectance of the optimized coating remains very low, less than 0.22%, over a wide angle range of 0°–75°. The maximum

value over the entire angle range is only 1.59%. The results show that the optimized AR coating is quite effective in reducing reflectivity over wide-angle and broadband ranges.

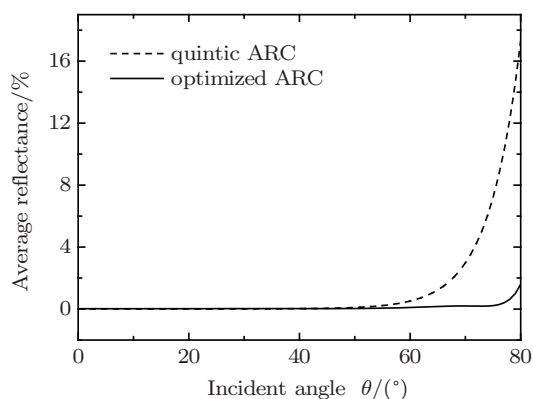


Fig. 3. Comparison of the average visible spectral reflectances of a quintic AR coating and the optimized GRIN AR coating versus incident angle.

2.2. Step-graded GRIN AR coating

In the following, we investigate the optimization design of step-graded GRIN coatings. The total thickness of the AR coating is an important parameter in the design process. We limit the total physical thickness to not more than $0.8 \mu\text{m}$. The step-graded GRIN AR coatings are optimized for wavelengths between 400 and 800 nm with 2 nm increments and incidence angles from 0° to 80° by steps of 2° . The lowest allowed refractive index is a critical factor in the design of broadband and wide-angle GRIN AR coatings. The inclusion of layers with a refractive index very close to that of air can greatly reduce reflection. When the minimal refractive index is restricted to 1.05, which is the lowest value so far reported,^[21] the average angle- and wavelength-averaged reflectance of the optimized three-layer AR coating is only 0.45%. In view of the difficulty of fabrication, the minimum refractive index of discrete layers in the following optimization process is restricted to $n_{\min} = 1.10$. However, this leads to an increment in the average reflectance of the optimized AR coating. The maximum allowed refractive index is set to 1.52. The calculated angle- and wavelength-averaged reflectance and the total thickness as a function of the number of steps for optimized coatings are shown in Fig. 4. As can be seen, the average reflectance initially decreases rapidly as more layers are added, and then becomes almost constant. Adding layers beyond two layers provides little benefit in reducing the average reflectance. The average reflectances of the two- and three-layer antireflection coatings are 1.32% and 1.2%, respectively. Compared to the optimized two-layer coating, the total thickness of the three-layer coating, however, increases from 325.5 nm to 415.7 nm. It can be seen that the two-layer GRIN AR coating with a smaller physical thickness reduces reflection effectively. The

fabrication process is much easier due to the simple structure with only two layers.

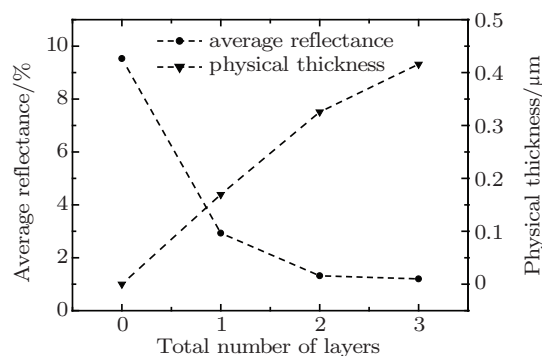


Fig. 4. Average reflectance and total physical thickness of step-graded GRIN AR coatings as a function of the step-number.

Table 1. Physical thickness and refractive index of each layer in the optimized two-layer GRIN AR coating.

Layer/nm	Refractive index	Thickness/nm
1	1.31	118.8
2	1.10	206.7

Table 1 shows the parameters of the two layers for the optimized two-layer coating. The layer with a 118.8 nm-thickness and refractive index of 1.31 is chosen as the first layer of the two-layer structure. The refractive index of the second layer is as low as 1.10, close to that of air.

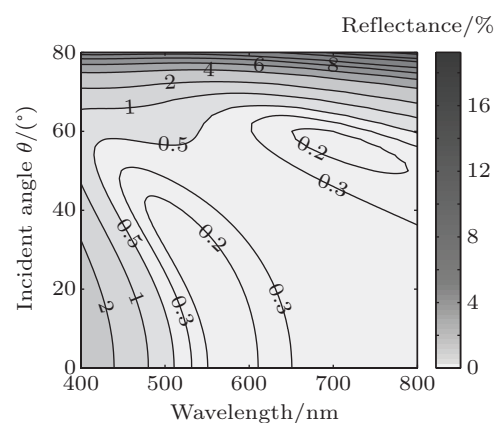


Fig. 5. Wide-angle and broadband AR performance of the two-layer discrete GRIN AR coating.

The simulated angle- and wavelength-reflection characteristic of an optimized two-layer GRIN AR coating is shown in Fig. 5. The average reflectance over the 400 nm–800 nm range and wide incident angle 0° – 80° is reduced to only 1.32% as compared to 9.53% for the BK7 glass substrate with no AR coating. This two-layer AR coating exhibits a very low average reflectance of $R \sim 0.323\%$ over a broad ranges of wavelengths, ($\lambda = 500 \text{ nm} - 800 \text{ nm}$) and incident angles ($\theta = 0^\circ - 60^\circ$).

3. Experiment

3.1. Preparation

The two-step GRIN AR coating discussed above was deposited onto a BK7 glass using electron beam evaporation with the GLAD technique. The low-refractive-index SiO₂ materials were evaporated from an EB source in the preparation of the two layers. The background pressure was 2.0×10^{-3} Pa, and the O₂ pressure was 1.0×10^{-2} Pa. The distance between the evaporation sources and the substrate was 27 cm. The BK7 glass ($\phi 30 \text{ mm} \times 1 \text{ mm}$) substrates were cleaned by acetone and ethanol before being introduced into the vacuum system. The change in glancing angle was controlled by a stepping motor. During the deposition process, the substrate was kept at room temperature. The film thickness was controlled by quartz crystal deposition monitor technology. Several nanostructured SiO₂ films were deposited under different glancing angles of 0, 30, 40, 50, 60, 70, 80, and 87°. The effective refractive indices ($\lambda=600 \text{ nm}$) of the samples are presented in Fig. 6. As can be seen, the value decreases with the increase in glancing angle. The refractive index of porous SiO₂ films decreases to 1.10 at a glancing angle of 87°, which is much lower than that of the corresponding bulk material. The relation between the refractive index and the glancing angle is fitted to a polynomial expression as

$$n(\theta) = 1.47124 + 1.13 \times 10^{-3} \times \theta - 3 \times 10^{-5} \times \theta^2 - 3.6634 \times 10^{-7} \times \theta^3. \quad (3)$$

From the above polynomial expression, we know that the minimum refractive index is 1.063 at an oblique angle of 90°. The glancing angle corresponding to the refractive index of 1.31 is about 66°.

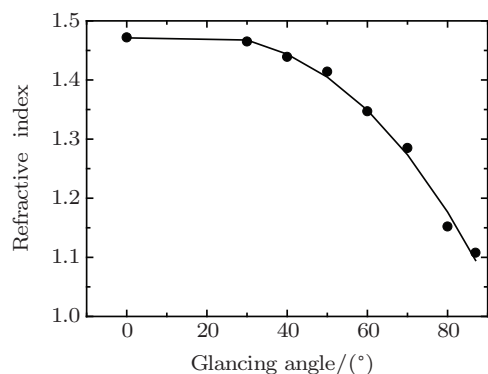


Fig. 6. Experimental data (dots) and curve fitting (solid line) of the refractive index versus deposition angle.

It is known that the distances between the evaporation source and different positions of the substrate are different in the preparation process with glancing angle deposition technology. This leads to nonuniform thickness of the obliquely

deposited film, especially at large deposition angles. The inhomogeneity will introduce errors into the measurement accuracy of the reflection spectrum of the sample. In order to improve the positional homogeneity, we adopted a method that has been used to prepare optical retardation plates.^[22] The substrate was rotated 180 degrees when the central thickness of the coating reached one-half the designed thickness. Then, the other half of the coating was deposited from the opposite direction. Theoretical results show that this bilayered film with good positional homogeneity has the same optical property as a coating that is deposited at a single angle. The designed AR structure was fabricated with deposition angles of 66°, -66°, 87°, and -87°, separately.

3.2. Results and discussion

The scanning electron micrograph (SEM) pattern of the sample is shown in Fig. 7. The bottom two layers with the symmetrical columnar structures are regarded as the “first” layer of the designed coating. The top two layers as the “second” layer are a mixture of slanted columnar structures and many voids. Both the column diameters and the gaps between the columnar structures are also much smaller than the wavelength of visible light. Therefore, the coating can keep the optical scattering sufficiently small.

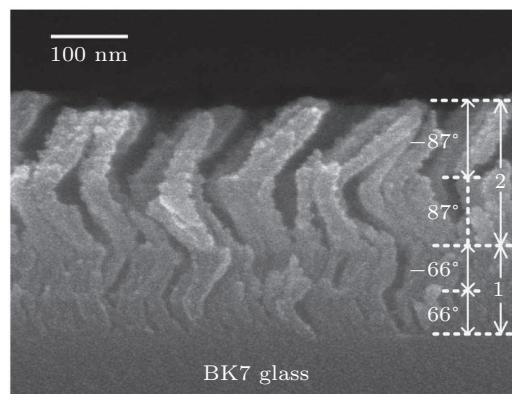


Fig. 7. Scanning electron micrograph of the graded-index AR coating.

The reflectance spectra were measured for wavelengths from 400 nm to 800 nm at 2 nm steps and for incident angles between 10° and 50°, in 2° increments, due to the limitation of the measuring instrument. As shown in Fig. 8, the measured reflectances basically fit the theoretical calculated results. The average reflection of the sample is 0.88% over the measured wavelength and incident angle ranges, which is close to the calculated value of 0.49%. Generally speaking, the measurement results demonstrate that the two-layer GRIN AR coating has excellent broadband and wide-angle antireflection characteristics.

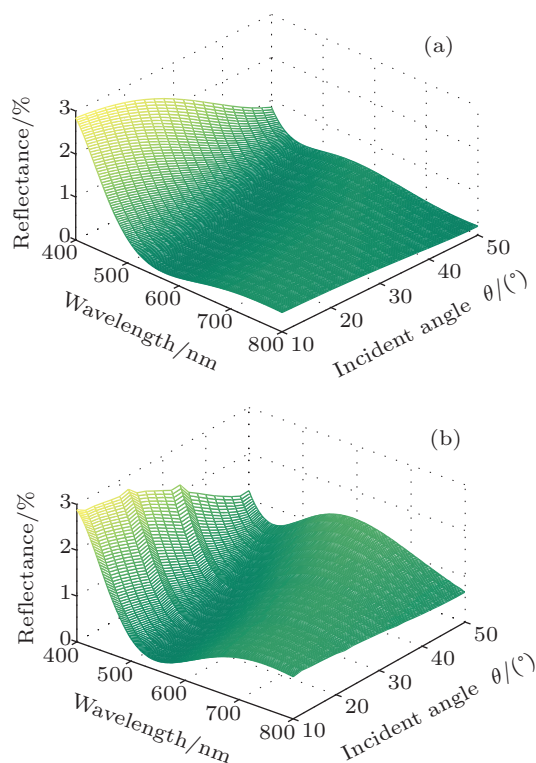


Fig. 8. (color online) (a) Calculated and (b) measured reflectivity of the optimized two-layer graded-index coating over angles of incidence 10–50° and wavelength range 400–800 nm.

4. Conclusions

A new method for the optimization of the refractive-index profile of wide-angle and broadband GRIN AR coatings is presented. The average reflectance of the designed AR coating over a wavelength range from 400 nm to 800 nm and angles of incidence from 0° to 80° is as small as 0.1%. Based on the limit of the lowest refractive index ($n_{\min} = 1.10$), the relation between the average reflection of the step-graded GRIN AR coatings and the step-number is studied. The average reflectance initially decreases rapidly as more layers are added, and then becomes almost constant. The two-layer coating with a simple structure and thin thickness of 325.5 nm can re-

duce the reflection to 1.32% for the wavelength range covering 400 nm to 800 nm and incident angles from 0° to 80°. Furthermore, the two-layer AR coating was fabricated by the glancing angle deposition technique. The average value of the measured reflectances is 0.88% over a broad spectrum, $\lambda = 400$ nm–800 nm, and a wide range of incident angles, $\theta = 10^\circ$ –50°. It is shown that the reflectances for the two-layer AR coating are in agreement with the theoretical results in the measured range.

References

- [1] Diedenhofen S L, Vecchi G, Algra R E, Hartsuiker A, Muskens O L, Immink G, Bakkens E P A M, Vos W L and Rivas J G 2009 *Adv. Mater.* **21** 973
- [2] Southwell W H 1985 *Appl. Opt.* **24** 457
- [3] Kong W J, Shen Z C, Wang S H, Shao J D, Fan Z X and Lu C J 2010 *Chin. Phys. B* **19** 044210
- [4] Zhang J C, Fang M, Jin Y X and He H B 2012 *Chin. Phys. B* **21** 014202
- [5] Southwell W H 1983 *Opt. Lett.* **8** 584
- [6] Fu X Y, Wang S M, Deng D G, Yi K, Shao J D and Fan Z X 2005 *Chin. Phys. Lett.* **22** 3173
- [7] Spiller E, Haller I, Feder R, Baglin J E E and Hammer W N 1980 *Appl. Opt.* **19** 3022
- [8] Fahr S, Ulbrich C, Kirchartz T, Rau U, Rockstuhl C and Lederer F 2008 *Opt. Express* **16** 9332
- [9] Mahdjoub A and Zighed L 2005 *Thin Solid Films* **478** 299
- [10] Kuo M L, Poxson D J, Kim Y S, Mont F W, Kim J K, Schubert E F and Lin S Y 2008 *Opt. Lett.* **33** 2527
- [11] Chhajed S, Schubert M F, Kim J K and Schubert E F 2008 *Appl. Phys. Lett.* **93** 251108
- [12] Lee C C, Tang C J and Wu J Y 2006 *Appl. Opt.* **45** 1333
- [13] Bartzsch H, Lange S, Frach P and Goedicke K 2004 *Surf. Coat. Technol.* **180** 616
- [14] Xiao X D, Dong G P, Xu C, He H B, Qi H J, Fan Z X and Shao J D 2008 *Appl. Surf. Sci.* **255** 2192
- [15] Popta A C, Hawkeye M M, Sit J C and Brett M J 2004 *Opt. Lett.* **29** 2545
- [16] Xi J Q, Schubert M F, Kim J K, Schubert E F, Chen M, Lin S Y, Liu W and Smart J A 2007 *Nat. Photonics* **1** 176
- [17] Greiner H 1996 *Appl. Opt.* **35** 5477
- [18] Yang J M and Kao C Y 2001 *J. Lightwave Technol.* **19** 559
- [19] Martin S, Rivory J and Schoenauer M 1995 *Appl. Opt.* **34** 2247
- [20] Schubert M F, Mont F W, Chhajed S, Poxson D J, Kim J K and Schubert E F 2008 *Opt. Express* **16** 5290
- [21] Schubert E F, Kim J K and Xi J Q 2007 *Phys. Status Solidi B* **244** 3002
- [22] Motohiro T and Taga Y 1989 *Appl. Opt.* **28** 2466